Supplementary Information for "Giant photocaloric effects across a vast temperature range in ferroelectric perovskites"

Riccardo Rurali

Institut de Ciència de Materials de Barcelona, ICMAB–CSIC, Campus UAB, 08193 Bellaterra, Spain

Carlos Escorihuela-Sayalero, Josep Lluís Tamarit, and Claudio Cazorla

Group of Characterization of Materials, Departament de Física, Universitat Politècnica de Catalunya, Campus Diagonal-Besòs, Av. Eduard Maristany 10–14, 08019 Barcelona, Spain and Research Center in Multiscale Science and Engineering, Universitat Politècnica de Catalunya, Campus Diagonal-Besòs, Av. Eduard Maristany 10–14, 08019 Barcelona, Spain

Jorge Íñiguez-González

Luxembourg Institute of Science and Technology (LIST), Avenue des Hauts-Fourneaux 5, L-4362 Esch/Alzette, Luxembourg and Department of Physics and Materials Science, University of Luxembourg, 41 Rue du Brill, L-4422 Belvaux, Luxembourg

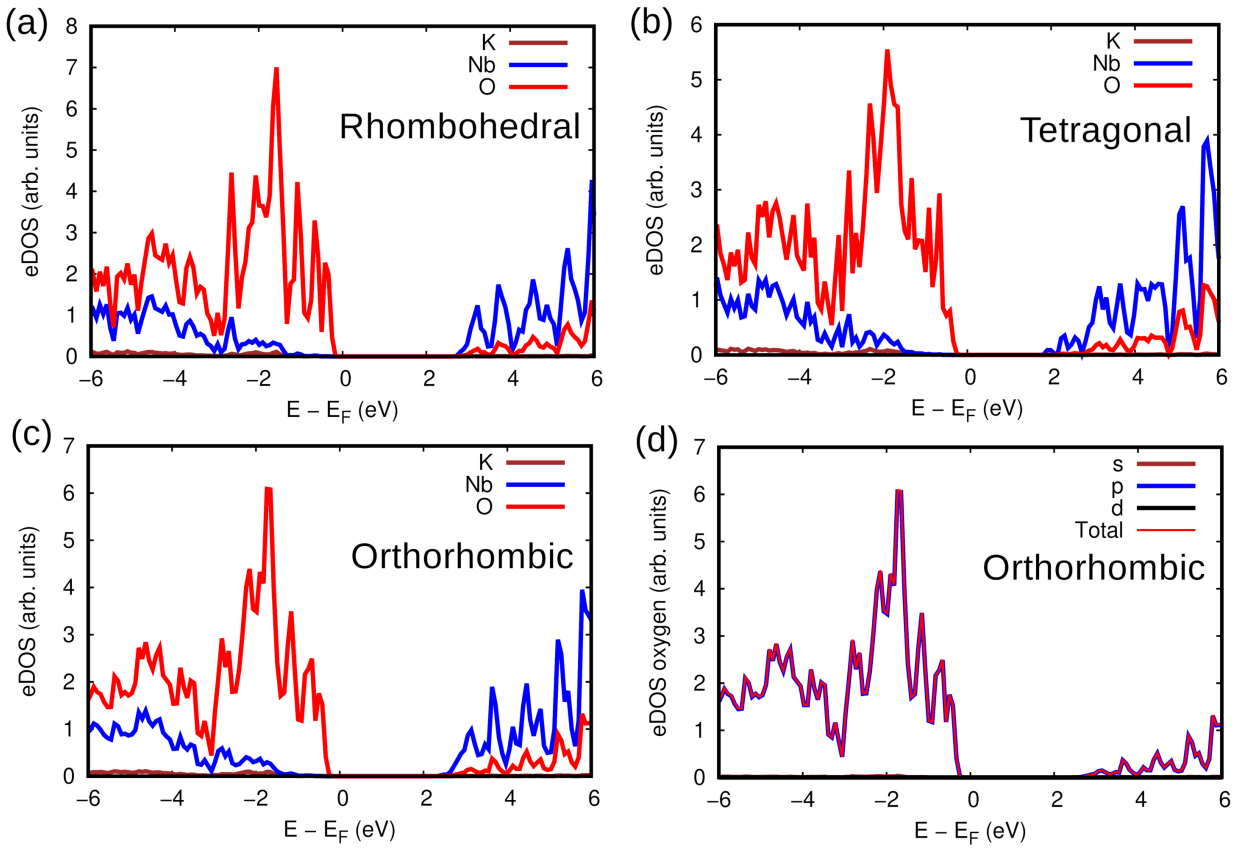

Supplementary Figure 1: Projected density of electronic states calculated for the three ferroelectric phases of $KNbO_3$. (a) Rhombohedral, (b) tetragonal and (c) orthorhombic phases. The energy band gap of the tetragonal phase is slightly smaller than that of the rhombohedral and orthorhombic phases. (d) Density of electronic valence states calculated for the oxygen atoms in the room-temperature polar orthorhombic phase. These oxygen valence states entirely present $2p$ orbital character.

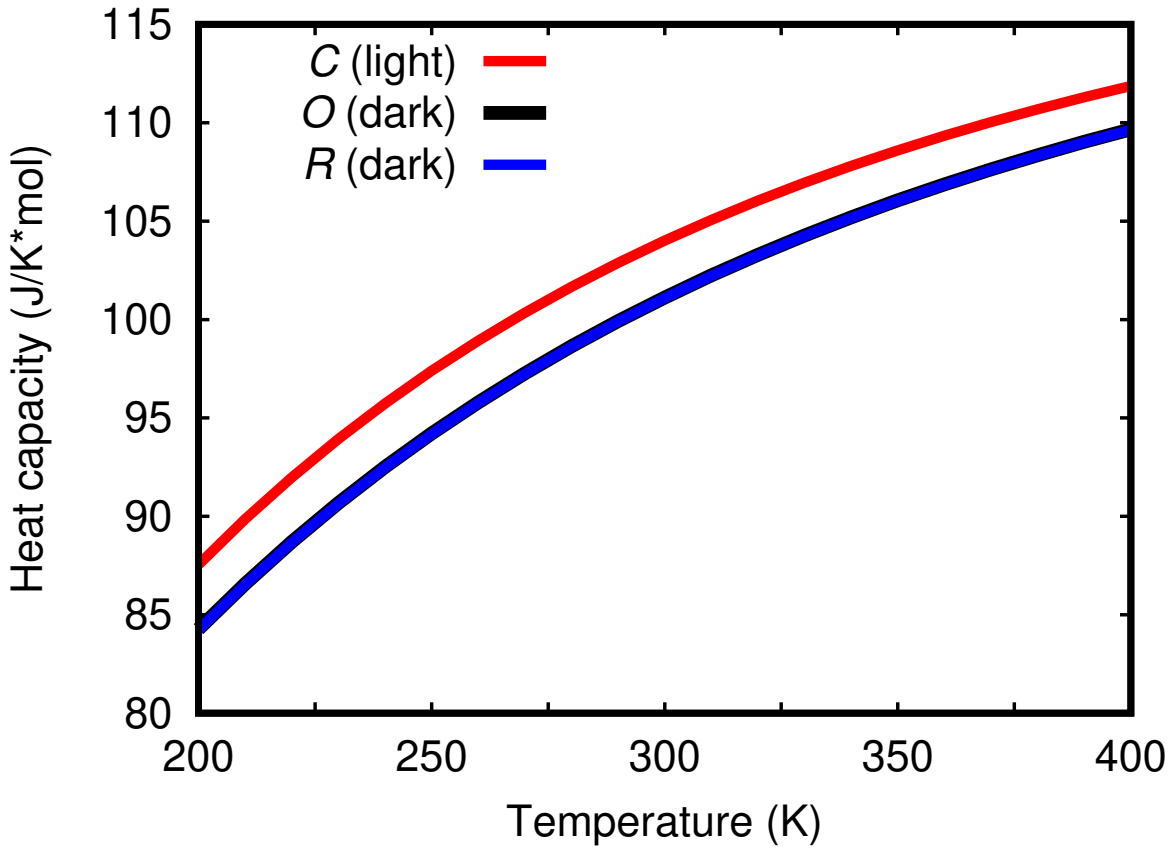

Supplementary Figure 2: Heat capacity of $KNbO_3$ estimated for the ferroelectric rhombohedral and ferroelectric orthorhombic phases under dark conditions and for the non-polar cubic phase stabilized by light. Calculations were performed within the quasi-harmonic approximation, that is, taking into account thermal expansion effects, and considering T-renormalized phonons for the room-temperature polar orthorhombic phase (DFT-rQHA). The heat capacity of the two polar R and O phases is practically identical (the corresponding curves are superimposed).

SUPPLEMENTARY METHODS

We performed density functional theory (DFT) calculations[1] with the projector augmented wave method[2] and generalized-gradient PBEsol approximation[3] (energy cutoff of 650 eV). The electrons treated as valence were: K $4s^1$ $3p^6$ $3s^2$, Nb $4d^4$ $5s^1$ $4p^6$, and O $2p^4$ $2s^2$. The first Brillouin zone (BZ) was sampled with a $12 \times 12 \times 12$ **k**-points grid and the atomic positions were optimized until the atomic forces were smaller than 0.5 meV Å^{-1}. Electric polarizations were calculated within a linear approximation using Born effective charges[4].

Photoexcitation was mimicked by constraining the partial occupancies of the electronic orbitals through adjustment of the Fermi distribution smearing. This effective DFT approach is effectively equivalent to those employed in previous works where the concentration of electron-hole pairs was constrained via the introduction of two adjustable quasi-Fermi levels[5–7].

The second-order interatomic force constants were computed by finite differences with Phonopy[8] using $5 \times 5 \times 5$ supercells for the polar phases and $4 \times 4 \times 4$ supercells for the nonpolar phase. Thermal expansion effects were appropriately accounted for with the quasi-harmonic approximation (QHA)[9].

The DynaPhoPy code[10] was used to calculate the anharmonic lattice dynamics of the room-temperature polar phase (T-renormalized phonons) from *ab initio* molecular dynamics (AIMD) simulations. DFT Gibbs free energies, G, and entropies, S, were computed with the QHA method considering T-renormalized phonons for the phases that are dynamically unstable at zero-temperature conditions ("DFT-rQHA"). AIMD simulations were carried out in the (N, V, T) ensemble at $T = 300$ K using Nosé-Hoover thermostats. A large simulation cell containing $N = 625$ atoms was employed with periodic boundary conditions applied along the three Cartesian directions. Newton's equations of motion were integrated using the customary Verlet's algorithm with a time step of $1.5 \cdot 10^{-3}$ ps. Γ-point sampling was used for BZ integration and the total duration of the AIMD simulations was of 60 ps.

SUPPLEMENTARY DISCUSSION

Next, we present an extensive discussion on several possible practical aspects affecting the implementation of the *photocaloric* effect unveiled in this study for solid-state cooling purposes. Since this is a newly predicted caloric effect and our expertise is neither in applied physics nor engineering, the discussion may be somewhat qualitative and conjectural at certain points.

1. Light penetration depth in $KNbO_3$

A comprehensive literature search was performed but we did not find any direct experimental measurements of the light penetration length in $KNbO_3$. However, for the extensively investigated and analogous ferroelectric oxide perovskite $BaTiO_3$, several experimental studies have reported this light penetration length to be 10–20 μm[11,12]. Therefore, it is reasonable to expect a similar light penetration length for $KNbO_3$, which is consistent with our indirectly estimated value of 30 μm. The technique employed in these light absorption coefficient experiments is spectrophotometry, performed with several Ar and HeNe laser beams.

2. Other possible factors affecting the degree of homogeneity of the light-induced ferroelectric to paraelectric phase transition in $KNbO_3$

In practice, the homogeneity of light-induced phase transitions may be affected by various factors beyond light penetration depth. For example, inhomogeneous excitation profiles generated by the pump beam within the material, as well as intrinsic heterogeneities such as surface roughness, interface effects, and defects, may impact the homogeneity of these transitions (see, for instance, work[13]). However, assessing these practical aspects, which may strongly depend on the specific experimental setup and sample preparation method, is beyond the scope of this theoretical and computational work.

3. Estimation of the light energy necessary to induce the ferroelectric to paraelectric phase transition in $KNbO_3$

One can roughly estimate the light energy necessary to trigger the ferroelectric to paraelectric phase transition in $KNbO_3$, U_{light}, which underpins the simple photocaloric cooling cycle

proposed in our article (Figure 5b in the main text). We start by considering that (1) the threshold conduction electronic density, according to our DFT calculations, necessary to trigger the light-induced phase transition is of the order of 10^{21} e^-/cm^3, and (2) the energy band gap of $KNbO_3$ and similar dielectric materials is of the order of 1 eV. Using these numbers, we estimate $u_{light} \sim 10^2$ J/cm^3.

Now, let us consider a thin film with typical dimensions of 1 cm $\times$ 1 cm surface and 1 μm $= 10^{-4}$ cm thickness, leading to a thin film volume $V_{tf} \sim 10^{-4}$ cm^3. Finally, we have $U_{light} = u_{light} \cdot V_{tf} \sim 10^2 \cdot 10^{-4} \sim 10^{-2}$ J, which turns out to be of the order of 10 mJ.

A more convenient quantity for assessing practical feasibility is the equivalent light energy surface density, which would amount to $\mu_{light} \sim 10$ mJ/cm^2 and in principle seems reasonable for practical applications. The corresponding irradiance, or light power per unit area, would depend on the specific electronic de-excitation rates in $KNbO_3$, which to the best of our knowledge have not been reported in the literature and in any case may strongly depend on the sample preparation conditions (e.g., concentration of point defects).

4. Heating produced by light absorption: how this would affect the proposed photocaloric cooling?

We honestly do not know the answer to this question right now. Addressing this question quantitatively would require very complex calculations beyond the scope of the present work. We would need to understand, for example, the specific electronic excitation and de-excitation processes occurring in $KNbO_3$, which, to the best of our knowledge, have not been reported in the literature. Additionally, we would need to know about the specific light-phonon and electron-phonon scattering processes occurring in $KNbO_3$ to estimate likely relaxation and heat transport mechanisms. However, as mentioned above, such calculations are beyond the scope of the present proof-of-concept study. The only way to confidently answer this question is to perform the actual experiments, which we aim to motivate with this theoretical work.

It is worth noting that, as a highly speculative possibility, the cycling rate of the four-step solid-state refrigeration cycle proposed in the main text could potentially be adjusted to match the characteristic electron-hole recombination rates in $KNbO_3$. This adjustment could compensate for likely non-radiative deexcitation processes. However, we are uncertain whether this is feasible in practice and do not know the specific characteristic electron-hole

recombination rates in $KNbO_3$.

Despite this lack of practical anticipation, we should mention that recently, optical control of electrical polarization has been experimentally demonstrated in several ferroelectric materials similar to $KNbO_3$. For instance, optically controlled reversal of the polarization and domain motion in $BaTiO_3$ and $LiNbO_3$[14], with promising prospects for ferroelectric memory applications, and optically induced appearance of polar order in strained $SrTiO_3$[15,16], suggestive of exotic photoflexoelectric couplings. These successful realizations of optical control of electrical polarization in oxide perovskites, where *a priori* heating of the samples could have also been an impeding factor, give us confidence in the likely practical viability of the photocaloric cooling strategy proposed in this study.

5. Is the direction of the electric polarization relevant for photo-cooling purposes?

For present photocaloric purposes, the direction of the polarization in principle should be irrelevant (i.e., assuming the absence of significant depolarization field effects in polydomain ferroelectric thin films). This is because rather than pursuing any specific functionality from the ferroelectric order parameter (such as switching the polarization with an external electric field for writing or reading information), we are primarily interested in the thermodynamics of the underlying ferroelectric to paraelectric phase transition. Specifically, the change in entropy associated with the light-induced phase transition needs to be substantial (that is, of the order of 10–100 J/K·kg) in order to efficiently remove heat from a cold source and transfer it to a hot end.

Having said this, for the specific case of monodomain ferroelectric thin films, where depolarization field effects may be substantial, the direction of the polarization should be in-plane. This orientation is necessary to prevent hindrance of the ferroelectric polarization caused by the accumulation of charges on the thin film surfaces.

6. The polar tetragonal phase in $KNbO_3$, is this phase relevant for ambient photo-cooling purposes?

Although in $KNbO_3$ under dark conditions the ferroelectric tetragonal phase appears closer in temperature to the high-temperature non-polar cubic phase than the ferroelectric rhombohedral and orthorhombic phases analyzed in the present study, for present near-ambient refrigeration purposes that ferroelectric tetragonal phase is not of interest for two

reasons. Firstly, in $KNbO_3$ the ferroelectric tetragonal phase is stabilized at temperatures significantly higher than room temperature, approximately 500 K, making it impractical for near-room-temperature refrigeration applications. Secondly, the electronic band gap of the ferroelectric tetragonal phase is quite similar in size to those of the ferroelectric orthorhombic and rhombohedral phases, approximately 3 eV (as explicitly shown in the Supplementary Figure 1). Thus, in principle, to a first approximation, the light energy necessary to excite electrons from the valence to the conduction band to trigger the ferroelectric to paraelectric phase transition would be very similar to that in the other two low-temperature phases. It is noted that this assumption has been explicitly ascertained in this study for the ferroelectric rhombohedral and ferroelectric orthorhombic phases, where the estimated threshold photoexcited carrier density for triggering the ferroelectric to paraelectric phase transition is the same (that is, indenpendently of their different stabilization temperature under dark conditions).

7. What is the estimated coefficient of performance (COP) of the proposed photocaloric cooling cycle?

One can roughly estimate the amount of light energy necessary to induce the ferroelectric to paraelectric phase transition in $KNbO_3$ per kilogram of substance, W. We start by considering that (1) the threshold conduction electronic density, according to our DFT calculations, necessary to trigger the light-induced phase transition is of the order of 10^{21} e^-/cm^3, (2) the energy band gap of $KNbO_3$ and similar dielectric materials is of the order of 1 eV, and (3) the density of $KNbO_3$ and similar dielectric materials is of the order 10 grams per cm^3. Using these numbers, we obtain that W is of the order of 10 kJ/kg. Considering that the amount of heat that can be removed in one PC cycle, Q, is of the order of 10 kJ/kg (that is, equal to $T \cdot \Delta S_{\text{PC}}$), we conclude that the COP associated with the predicted photocaloric effect, equal to Q/W, is of the order of 1. This value, although promising for solid-state cooling applications, is not competitive yet with present commercial air conditioning systems based on gas compression/decompression cycles, which typically present COP of the order of 10.

Nevertheless, as explained in the main text of the manuscript, the most interesting practical features of the predicted photocaloric effects are their size scalability (e.g., down to electronic devices dimensions) and vast temperature operation interval (i.e., several hundreds of degrees Kelvin), both of which do not apply to commercial air conditioning

systems. Furthermore, future engineering developments will likely achieve substantial improvements in the estimated COP, as is for other more mature solid-state cooling technologies (see, for instance, work[17]).

SUPPLEMENTARY REFERENCES

[1] G. Kresse and J. Furthmüller, Phys. Rev. B **54**, 11169 (1996).

[2] P. E. Blöchl, Phys. Rev. B **50**, 17953 (1994).

[3] J. P. Perdew, A. Ruzsinszky, G. I. Csonka *et al.*, Phys. Rev. Lett. **100**, 136406 (2008).

[4] C. Menéndez and C. Cazorla, Phys. Rev. Lett. **125**, 17601 (2020).

[5] C. Paillard, E. Torun, L. Wirtz, J. Íñiguez and L. Bellaiche, Phys. Rev. Lett. **123**, 087601 (2019).

[6] B. Peng, Y. Hu and S. Murakami *et al.*, Sci. Adv. **6**, eabd1618 (2020).

[7] C. Cazorla, S. Bichelmaier, C. Escorihuela-Sayalero *et al.*, Nanoscale **16**, 8335 (2024).

[8] A. Togo and I. Tanaka, Scr. Mater **108**, 1 (2015)

[9] C. Cazorla and J. Boronat, Rev. Mod. Phys. **89**, 035003 (2017).

[10] A. Carreras, A. Togo and I. Tanaka, Comput. Phys. Commun. **221**, 221 (2017).

[11] G. Ross, G. Montemezzani, P. Bernasconi, M. Zgonik and P. Günter, J. Appl. Phys. **79**, 3665 (1996).

[12] G. S. Garcia Quirino, J. J. Sanchez-Mondragon and S. Stepanov, Phys. Rev. A **51**, 1571 (1995).

[13] A. S. Johnson, D. Perez-Salinas, K. M. Siddiqui *et al.*, Nat. Phys. **19**, 215 (2023).

[14] R. Mankowsky, A. von Hoegen, M. Först and A. Cavalleri, Phys. Rev. Lett. **118**, 197601 (2017).

[15] X. Li, T. Qiu, J. Zhang *et al.*, Science **364**, 1079 (2019).

[16] T. F. Nova, A. S. Disa, M. Fechner *et al.*, Science **364**, 1075 (2019).

[17] P. M. Resende, F. Le Goupil, G. Fleury and G. Hadziioannou, Phys. Rev. Applied **21**, 054021 (2024).